Electronic Supplementary Material (ESI) for Molecular BioSystems.
This journal is © The Royal Society of Chemistry 2015

Figure S1

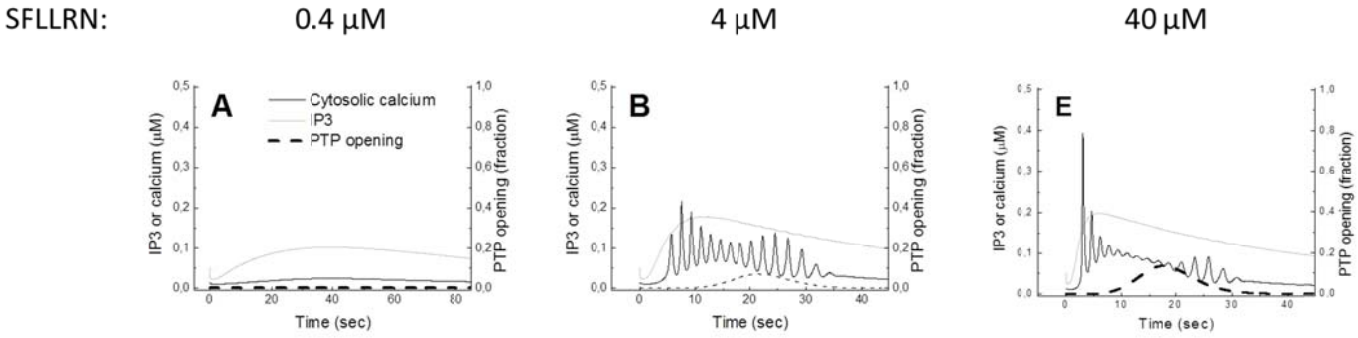

Fig. S1. Responses in platelet signaling obtained in the model in deterministic simulation. The panels show results of deterministic simulations for platelets stimulated with SFLLRN at (A) 0.4 μM, (B) 4 μM, or (C) 40 μM. Low SFLLRN concentration leads to sustained low cytosolic calcium level; its increase results in oscillations; further activator increase induces sustained increase in cytosolic calcium for 20 sec.

Figure S2

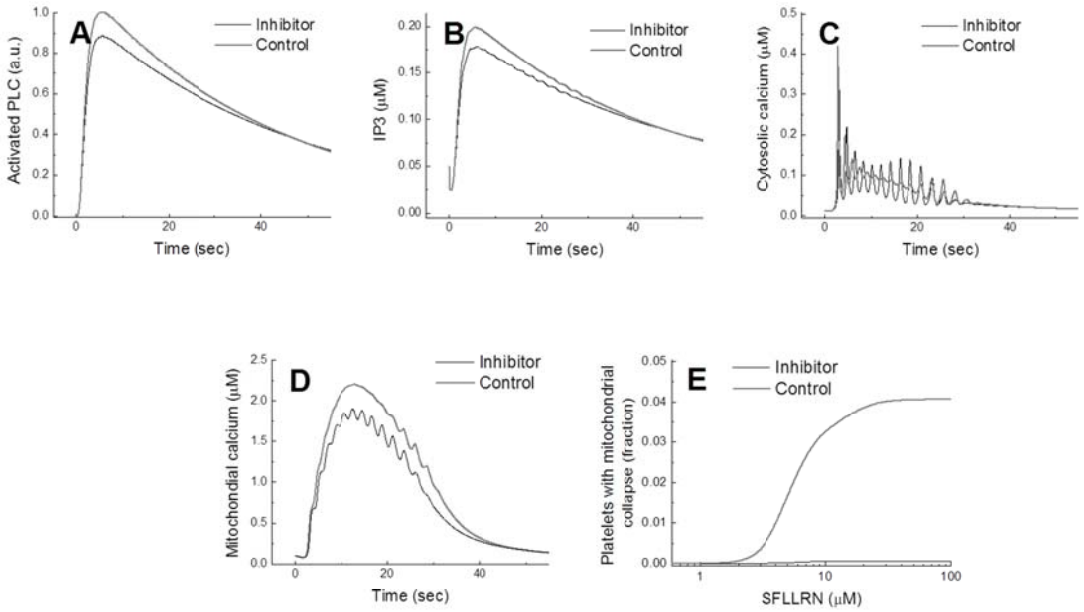

Fig. S2. Influence of PLC inhibition on platelet calcium signaling. A hypothetic PLC inhibitor with K_I of 10,000 molecules per platelet. The panels (A-D) show results of deterministic simulations for platelets stimulated with 100 μM of SFLLRN with (black curves) or without (grey curves) the PLC inhibitor ($9 \cdot 10^5$ molecules per platelet give an approximately 10% inhibition). (E) Fraction of platelets with the opened pore as a function of SFLLRN concentration; heterogeneous platelet population was obtained by varying the number of IP3R (Gaussian distribution), deterministic calculations.

Figure S3

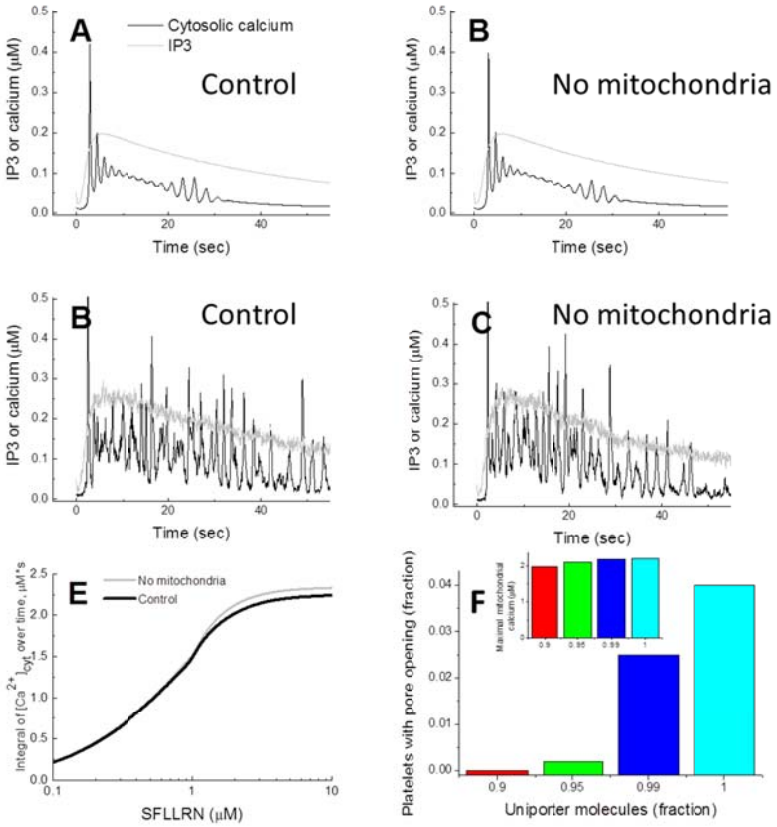

Fig. S3. Influence of mitochondria on platelet calcium signaling. The panels (A-D) show results of deterministic (A,B) or stochastic (C,D) simulations for platelets stimulated with 100 μM of SFLLRN with (A,C) or without (B,D) mitochondria uniporter. (E) Total calcium entrance into cytosol during 100 s after activation as a function of SFLLRN concentration, deterministic calculations. (F) Dependence of the fraction of platelets with the opened pore on the number of mitochondria uniporters, heterogeneous platelet population was obtained by varying the number of IP3R (Gaussian distribution), 100 μM of SFLLRN, deterministic calculations. Mitochondrial calcium uptake does not significantly influence cytosolic calcium concentration dynamics, yet it is vital for platelet subpopulation formation.

Figure S4

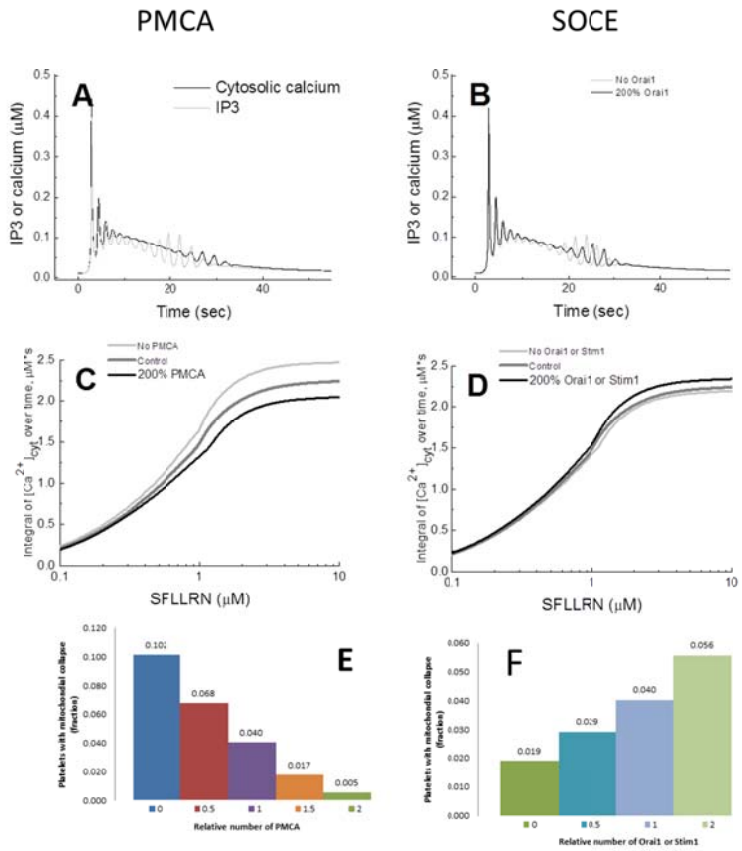

Fig. S4. Influence of the plasmatic membrane channels/pumps on platelet calcium signaling. (A, B) **R**esults of deterministic simulations for platelets stimulated with 100 μM of SFLLRN with varying amount of PMCA (A) or SOCE (B). (C, D) Total calcium entrance into cytosol during 100 s after activation as a function of SFLLRN concentration, deterministic calculations. (E, F) Dependence of the fraction of platelets with the opened pore on the relative number of PMCA (E) or SOCE channels (F), heterogeneous platelet population was obtained by varying the number of IP3R (Gaussian distribution), 100 μM of SFLLRN, deterministic calculations.

Figure S5

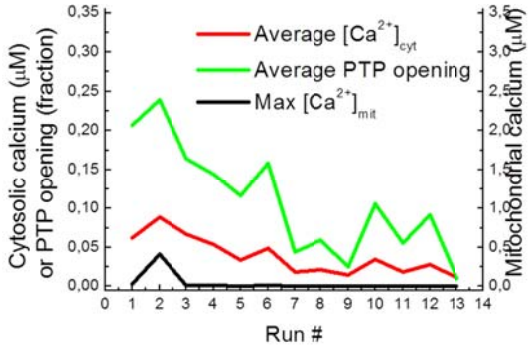

Fig. S5. Correlation between average concentration of calcium in cytosol, maximum concentration of calcium in mitochondria and average opening of mPTP in different stochastic runs. The concentration of SFLLRN was 4 μM in runs #1-4 and 0.4 μM in runs #5-13. The average and maximal values were calculated for 40 s of model time. Correlation between average cytosolic calcium and maximal mitochondrial calcium equals 0.97.

Figure S6

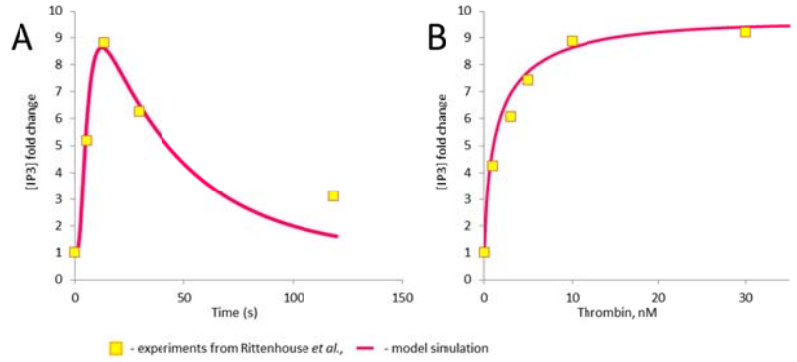

Fig. S6. IP3 generation in platelet after stimulation with thrombin in Module1 in comparison with experimental data. 1 nM of thrombin is considered to correspond to 0.4 µM of SFLLRN. (A) Dynamics of cytosolic IP3 concentration in response to stimulation with thrombin at 10 nM (SFLLRN at 4 µM). (B) Maximal IP3 increase as a function of thrombin or SFLLRN concentration. Experimental data are from J Biol Chem 1985; 260: 8657-8660.

Figure S7

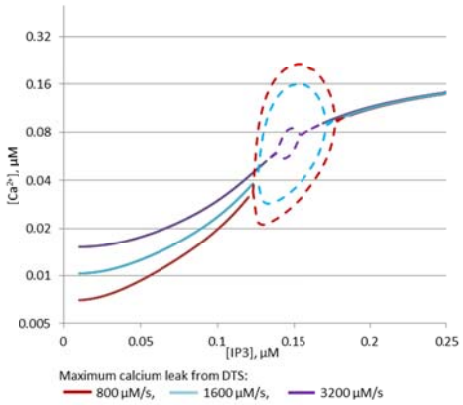

Fig. S7. Cytosolic calcium concentration after stimulation of Module 2 with constant [IP3]. Solid lines indicate steady states, dashed lines show the stable oscillation region. Increase of the DTS membrane leaks decrease the region of oscillation behavior.

Figure S8

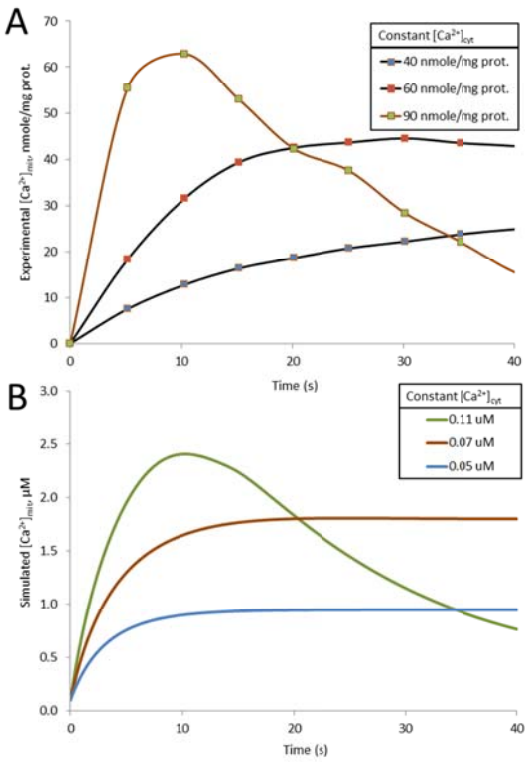

Fig. S8. Calcium concentration in the mitochondrial matrix in Module 3 after stimulation of mitochondria with constant cytosolic calcium concentration. (A) Experiments of Akopova et al. [Ukr.Biokhim Zh 2008; 80: 40-47], isolated mitochondria were stimulated with increasing concentrations of calcium in the medium (indicated in the legend) and amount of calcium in the mitochondrial matrix was measured. (B) Simulation of calcium accumulation in the mitochondria in module 3 of the model.

Supporting Tables

Table S1. Model equations

Module	Name	Reaction	Flux, compartment	Parameters	Ref.
PAR	Activation of PAR1	$PAR1 + Thr \leftrightarrow PAR1^*$	$k[PAR1][Thr] - k_m[PAR1^*]$, PM	$k = 0.03(nM \cdot s)^{-1}$, $k_m = 0.001s^{-1}$	[14]
PAR	Degradation of PAR1*	$PAR1^* \rightarrow$	$k[PAR1^*]$, PM	$k = 20s^{-1}$	[14], this work
PAR		$GqGTP \rightarrow GqGDP$	$k[GqGTP]$, PM	$k = 0.02s^{-1}$	[14]
PAR		$PLCGqGTP \rightarrow PLCGqGDP$	$k[PLCGqGTP]$, PM	$k = 15s^{-1}$	[14]
PAR		$PAR1^*Gq + GTP \leftrightarrow PAR1^*GqGTP$	$k[PAR1^*Gq][GTP] - k_m[PAR1^*GqGTP]$, PM	$k = 1(\mu M \cdot s)^{-1}$, $k_m = 0.1s^{-1}$	[14]
PAR		$PAR1^*Gq + GDP \leftrightarrow PAR1^*GqGDP$	$k[PAR1^*Gq][GDP] - k_m[PAR1^*GqGDP]$, PM	$k = 1(\mu M \cdot s)^{-1}$, $k_m = 5s^{-1}$	[14]
PAR		$PAR1^* + GqGDP \leftrightarrow PAR1^*GqGDP$	$k[PAR1^*][GqGDP] - k_m[PAR1^*GqGDP]$, PM	$k = 100(\mu M \cdot s)^{-1}$, $k_m = 1s^{-1}$	[14]
PAR		$PAR1^*GqGTP \rightarrow PAR1^* + GqGTP$	$k_m[PAR1^*GqGTP]$, PM	$k_m = 2s^{-1}$	[14]
PAR		$PLCGqGTPPIP2 \rightarrow PLCGqGTP + IP3$	$k[PLCGqGTPPIP2]$, PM	$k = 320s^{-1}$	[14]
PAR		$PLCGqGTP \leftrightarrow PLC + GqGTP$	$k[PLCGqGTP] - k_m[PLC][GqGTP]$, PM	$k = 5s^{-1}$, $k_m = 500(\mu M \cdot s)^{-1}$	[14]
PAR		$PLCGqGTPPIP2 \leftrightarrow PIP2 + PLCGqGTP$	$k[PLCGqGTPPIP2] - k_m[PIP2][PLCGqGTP]$, PM	$k = 1s^{-1}$, $k_m = 1000(\mu M \cdot s)^{-1}$	[14]
PAR		$PLCGqGDP \leftrightarrow PLC + GqGDP$	$k[PLCGqGDP] - k_m[PLC][GqGDP]$, PM	$k = 10^5 s^{-1}$, $k_m = 10^{-4}(\mu M \cdot s)^{-1}$	[14]
PAR	Simplified PI turnover	$IP3 \leftrightarrow PIP2$	$k[IP3] - k_m[PIP2]$, PM	$k = 0.17s^{-1}$, $k_m = 1.8 \cdot 10^{-5}s^{-1}$	This work
PM	Calcium PM leak	$Ca^{2+}_{ex} \leftrightarrow Ca^{2+}_{cyt}$	$\gamma ln\frac{[Ca^{2+}_{ex}]}{[Ca^{2+}_{cyt}]}$, cytosol	$\gamma = 11.3\ nM \cdot s^{-1}$	[16], this work
PM	PMCA	$Ca^{2+}_{cyt} \rightarrow Ca^{2+}_{ex}$	$\frac{V[Ca^{2+}_{cyt}]^2}{K^2+[Ca^{2+}_{cyt}]^2}$, cytosol	$V = 6\mu M \cdot s^{-1}$, $K = 0.05\mu M$	This work
DTS	SERCA2b	$Ca^{2+}_{cyt} \rightarrow Ca^{2+}_{dts}$	$\frac{V[Ca^{2+}_{cyt}]^{1.7}}{K^{1.7}+[Ca^{2+}_{cyt}]^{1.7}}$, cytosol	$V = 60mM \cdot s^{-1}$, $K = 0.27\mu M$	[27], this work
DTS	SERCA3	$Ca^{2+}_{cyt} \rightarrow Ca^{2+}_{dts}$	$\frac{V[Ca^{2+}_{cyt}]^{1.8}}{K^{1.8}+[Ca^{2+}_{cyt}]^{1.8}}$, cytosol	$V = 60mM \cdot s^{-1}$, $K = 1.1\mu M$	[27], this work
DTS	Calcium DTS leak	$Ca^{2+}_{dts} \leftrightarrow Ca^{2+}_{cyt}$	$\gamma ln\frac{[Ca^{2+}_{dts}]}{[Ca^{2+}_{cyt}]}$, cytosol	$\gamma = 21\mu M \cdot s^{-1}$	[16], this work
DTS	Calcium release thru IP3R	$Ca^{2+}_{dts} \rightarrow Ca^{2+}_{cyt}$	$\gamma P_0[IP3R]ln\frac{[Ca^{2+}_{dts}]}{[Ca^{2+}_{cyt}]}$, cytosol, $P_0 = \left(0.9\frac{[IP3Ra]}{[IP3R]} + 0.1\frac{[IP3Ro]}{[IP3R]}\right)^4$	$\gamma = 4.2 \cdot 10^5 s^{-1}$	[16]
DTS	IP3R	$IP3Ra \rightarrow IP3Ro + Ca^{2+}_{cyt}$	$\frac{k_1L_1[IP3Ra]}{L_1+[Ca^{2+}_{cyt}]}$, cytosol	$k_1 = 11.94s^{-1}$	[26]
DTS	IP3R	$IP3Ro + Ca^{2+}_{cyt} \rightarrow IP3Ra$	$\frac{(k_5L_5+K_5)[Ca^{2+}_{cyt}][IP3Ro]}{L_5+[Ca^{2+}_{cyt}]}$, cytosol	$k_5 = 4(\mu M \cdot s)^{-1}$, $K_5 = 4707s^{-1}$	[26]

DTS	IP3R	$IP3Ro \rightarrow IP3Rn + IP3$	$\frac{\left(K_3+k_{m3}\left[Ca_{cyt}^{2+}\right]\right)L_5[IP3Ro]}{L_5+\left[Ca_{cyt}^{2+}\right]}$, cytosol	$k_{m3} = 2.5(\mu M \cdot s)^{-1}$, $K_3 = 1.4s^{-1}$	[26]
DTS	IP3R	$IP3Rn + IP3 \rightarrow IP3Ro$	$\frac{\left(k_3L_3+k_{c3}\left[Ca_{cyt}^{2+}\right]\right)[IP3][IP3Rn]}{L_3+\left[Ca_{cyt}^{2+}\right]\left(1+\frac{L_3}{L_1}\right)}$, cytosol	$k_3 = 37.4(\mu M \cdot s)^{-1}$, $k_{c3} = 1.7(\mu M \cdot s)^{-1}$	[26]
DTS	IP3R	$IP3Ro \leftrightarrow IP3Rs$	$\frac{k_4L_5[IP3Ro]}{L_5+\left[Ca_{cyt}^{2+}\right]} - k_{m4}[IP3Rs]$, cytosol	$k_4 = 0.11s^{-1}$, $k_{m4} = 29.8s^{-1}$	[26]
DTS	IP3R	$IP3Rn + Ca_{cyt}^{2+} \leftrightarrow IP3Ri1$	$\frac{k_2\left[Ca_{cyt}^{2+}\right][IP3Rn]}{L_1+\left[Ca_{cyt}^{2+}\right]\left(1+\frac{L_1}{L_3}\right)} - k_{m2}[IP3Ri1]$, cytosol	$k_2 = 1.78s^{-1}$, $k_{m2} = 0.84s^{-1}$	[26]
DTS	IP3R	$IP3Ra + Ca_{cyt}^{2+} \leftrightarrow IP3Ri2$	$\frac{k_2\left[Ca_{cyt}^{2+}\right][IP3Ra]}{L_1+\left[Ca_{cyt}^{2+}\right]} - k_{m2}[IP3Ri2]$, cytosol		[26]
PM	SOCE	$Orai1\_closed \leftrightarrow Orai1\_opened$	$k[Orai1\_closed][Stim1] - k_m[Orai1\_opened]$, cytosol	$k = 1.226(\mu M \cdot s)^{-1}$, $k_m = 0.068s^{-1}$	[25]
DTS	SOCE	$Stim1 + 3\ Ca_{dts}^{2+} \leftrightarrow Stim1Ca$	$k[Stim1][Ca_{dts}^{2+}]^3 - k_m[Stim1Ca]$, DTS	$k = 667(mM^3 \cdot s)^{-1}$, $k_m = 2.535s^{-1}$	[25]
PM	SOCE	$Ca_{ex}^{2+} \leftrightarrow Ca_{cyt}^{2+}$	$\gamma[Orai1_{opened}]ln\frac{\left[Ca_{ex}^{2+}\right]}{\left[Ca_{cyt}^{2+}\right]}$, cytosol	$\gamma = 1.55\ \mu M \cdot s^{-1}$	This work
Mit (*)	NCLX	$Ca_{mit}^{2+} \rightarrow Ca_{cyt}^{2+}$	$\gamma\left(1+\frac{K}{\left[Ca_{mit}^{2+}\right]}\right)^{-1} e^{\frac{F(\Delta\psi-\Delta\psi*)}{2RT}}$, matrix	$\gamma = 1.84 \cdot 10^3 \mu M \cdot s^{-1}$, $K = 3\ \mu M$, $\Delta\psi^* = 0.091V$	[31]
Mit (*)	Uniporter	$Ca_{cyt}^{2+} \rightarrow Ca_{mit}^{2+}$	$\gamma\frac{\left[Ca_{cyt}^{2+}\right]}{K^2+\left[Ca_{cyt}^{2+}\right]^2}\frac{(\Delta\psi-\Delta\psi*)^3}{(\overline{\Delta\psi})^3+(\Delta\psi-\Delta\psi*)^3}\frac{\frac{2F\Delta\psi}{RT}\left(\left[Ca_{cyt}^{2+}\right]-\left[Ca_{mit}^{2+}\right]e^{-\frac{2F\Delta\psi}{RT}}\right)}{1-e^{-\frac{2F\Delta\psi}{RT}}}$, matrix	$\gamma = 64.2\mu M^2 \cdot s^{-1}$, $K = 0.07\ \mu M$, $\Delta\psi^* = 0.013V$, $\overline{\Delta\psi} = 0.124V$	[30]
Mit	Uniporter	$\Delta\psi \rightarrow$	$\gamma\frac{\left[Ca_{cyt}^{2+}\right]}{K^2+\left[Ca_{cyt}^{2+}\right]^2}\frac{(\Delta\psi-\Delta\psi*)^3}{(\overline{\Delta\psi})^3+(\Delta\psi-\Delta\psi*)^3}\frac{\frac{2F\Delta\psi}{RT}\left(\left[Ca_{cyt}^{2+}\right]-\left[Ca_{mit}^{2+}\right]e^{-\frac{2F\Delta\psi}{RT}}\right)}{1-e^{-\frac{2F\Delta\psi}{RT}}}$, matrix	$\gamma = 88.5mV \cdot \mu M \cdot s^{-1}$, $K = 0.07\ \mu M$, $\Delta\psi^* = 0.013V$, $\overline{\Delta\psi} = 0.124V$	[30]
Mit	NCLX	$\Delta\psi \rightarrow$	$\gamma\left(1+\frac{K}{\left[Ca_{mit}^{2+}\right]}\right)^{-1} e^{\frac{F(\Delta\psi-\Delta\psi*)}{2RT}}$, matrix	$\gamma = 1.27\ V \cdot s^{-1}$, $K = 3\ \mu M$, $\Delta\psi^* = 0.091V$	[31]
Mit	Respiratory chain	$\Delta\psi \leftrightarrow$	$\gamma e^{\frac{F(\Delta\psi)}{RT}} - Jres$, matrix	$\gamma = 17.3\ mV \cdot s^{-1}$, $Jres = 3.45\ V \cdot s^{-1}$	Adapted from [30]
Mit	mPTP	$mPTP_{opened} \leftrightarrow mPTP_{closed}$	$\frac{\gamma\left[mPTP_{opened}\right]}{1+e^{-\frac{(\Delta\psi-\Delta\psi*)}{\Delta\psi}}} - \frac{\left[Ca_{mit}^{2+}\right]^4[mPTP_{closed}]}{K^4+\left[Ca_{mit}^{2+}\right]^4}e^{-\frac{(\Delta\psi-\Delta\psi**)}{\overline{\Delta\psi}}}$, matrix	$\gamma = 0.397s^{-1}$, $K = 5\ \mu M$, $\Delta\psi^* = 0.091V, \overline{\Delta\psi} = 0.001V$, $\Delta\psi^{**} = 0.11V, \overline{\overline{\Delta\psi}} = 0.02V$	From [30] with modifications
Mit	mPTP	$\Delta\psi \rightarrow$	$\gamma\left[mPTP_{opened}\right]\frac{F(\Delta\psi)}{RT}\frac{e^{\frac{F(\Delta\psi)}{RT}}-e^{-\frac{F(\Delta\psi)}{RT}}}{1-e^{-\frac{F(\Delta\psi)}{RT}}}$, matrix	$\gamma = 0.138\ V \cdot s^{-1}$	[30]

(*) Calcium in mitochondria is highly buffered, so only 0.3% of calcium influx remains in the ion form [31]

Table S2. Sensitivity analysis of the model, parameters with non-zero sensitivities to stimulation with 1 μM of SFLLRN

Description	Value
SERCA 2b Hill coeficient	4.9054
IP3R activation constant l6	3.8324
IP3R equilibrium constant L5	-3.8195
IP3R activation constant lm6	-3.7972
SERCA2b half-activation constant ($K_{0.5}$)	2.9336
PIP2 turnover rate constant 1	-2.8707
IP3R binding IP3 constant *k2*	2.6599
IP3R release IP3 constant *km2*	-2.6127
PAR1* binding Gq rate constant	2.4062
Degradation of PAR1*	-2.4058
Number of SERCA2b copies per platelet	-1.9476
Number of IP3R copies per platelet	1.8587
Ca^{2+} flux through the IP3R channel	1.8522
PIP2 degradation rate constant	1.8139
IP3R activation constant l2	-1.325
IP3R activation constant lm2	1.3125
IP3R equilibrium constant L3	1.1165
PAR1 activation rate constant	1.0185
SERCA 3a Hill coeficient	0.7232
PLC binding PIP2 rate constant	0.6229
GTP hydrolysis by PLC rate constant	-0.6154
PIP2 turnover rate constant 2	0.4525
PAR1*Gq releasing GDP rate constant	0.4205

PAR1* releasing Gq rate constant	-0.4031
SERCA3a half-activation constant ($K_{0.5}$)	0.2536
IP3R activation constant l4	0.2488
IP3R activation constant lm4	-0.2239
IP3R equilibrium constant L1	0.2085
IP3R activation constant km4	-0.1805
IP3R activation constant k4	0.1773
Ca2+ flux through the DTS membrane	0.1218
IP3R activation constant km1	0.0649
IP3R activation constant k1	-0.0576
NCLX activation constant	0.0462
	0.0462
UNI activation constant	-0.044
PAR1*Gq binding GTP rate constant	0.0429
PLC binding GqGTP rate constant	0.0318
PMCA half-activation constant ($K_{0.5}$)	0.0287
Number of PM NCX copies per platelet	0.0273
PAR1* releasing GqGTP rate constant	0.0197
IP3R closing constant k1	0.0186
Buffering of Ca2+ in mitochondria	0.018
Ca2+ flux through the plasma membrane	0.018
Ca2+ leak trough PM	0.018
PMCA Hill coeficient	0.0175
GqGTP hydrolysis rate constant	-0.0173
Number of UNI copies per platelet	-0.0145
Mitochondrial inner membrane potential offset value	-0.0123

PLC releasing GqGDP rate constant	0.0109
Density of mitochondrial protein	0.0102
PLC releasing PIP2 rate constant	0.0099
Deactivation of Stim1	0.0089
Number of PM NCX	0.0082
PLC releasing GqGTP rate constant	-0.006
PAR1*Gq releasing GTP rate constant	0.0048
Mitochondrial respiratory chain electron flux	0.0047
IP3R closing constant k3	0.0042
Hydrogen leak trough UNI	0.0041
Activation of Stim1	0.0039
PAR1*Gq binding GDP rate constant	-0.0025
Number of mPTP per platelet	-0.0025
Number of PMCA copies per platelet	-0.0024
Leak of hydrogen ions through the mitochondria membrane	-0.0012
Leak of hydrogen ions through the mitochondria membrane	-0.0012
Ca2+ flux through Orai1	0.001
Orai1 opening	0.0006
Number of mitochondria per platelet	-0.0006
Orai1 closing	-0.0003
Hydrogen leak trough NCLX	0.0002
PLC binding GqGDP rate constant	0.0002